FOREST FIRE DETECTION BASED ON GAUSSIAN FIELD ANALYSIS

Florent Lafarge, Xavier Descombes, Josiane Zerubia

Ariana Reseach Group - INRIA
2004, routes des Lucioles, BP93
06902 Sophia Antipolis, Cedex France
E-mail=Name.Lastname@inria.fr

ABSTRACT

The Thermical InfraRed (TIR) channel contains wave lengths sensitive to the emission of heat. The forest fires can be characterized by intensity peaks on TIR images. We present a fully automatic method of forest fire detection from TIR satellite images based on the random field theory. First, preprocessing is used to model the image as a realization of a Gaussian field which presents interesting properties. The fire areas which are supposed to be a minority are considered as anomalies of that field. We present a statistical analysis of Gaussian field to determine a degree of belonging of a cluster to the image background (i.e. a realization of a Gaussian field). We then extend this application to the estimation of the fire propagation direction.

1. INTRODUCTION

The forest fires cause a lot of damage and participate to the deterioration of the Earth ecosystem, especially to the global warming. One of the main issues is to quickly locate them in an automatic way. With the recent progress in the spatial domain, this detection problem can nowadays be tackled through satellite images.
In this domain, various methods have been proposed. Most of them are based on radiometric analysis from Thermical InfraRed (TIR) images as the work of Flannigan and Vonder Haar [3]. Such algorithms allow to estimate the ground temperature and efficiently detect fires using thresholding techniques. Hybrid approaches have also been developed such as [7] where TIR data are coupled with varied kinds of information. Other works such as [6] try to detect the forest fires through the emitted smokes by using learning methods. However, most of these methods need either training sets or a priori knowledge concerning the used sensors or the observed areas.
We present a new method which does not use this kind of information. The proposed approach allows to automatically detect the forest fires from TIR satellite images. TIR channel contains wave lengths sensitive to the emission of heat. It means that forest fires can be characterized by intensity peaks on this kind of images. However, all intensity peaks of a TIR image are not necessary forest fires. The main difficulty, as we can see on Figure 1, consists in making the distinction between peaks due to fire and other peaks of the image background which can correspond to industrial activities for example. An anomaly detection method is proposed to achieve this distinction. Such an approach is particularly efficient to extract image irregularities, as it can be seen in [2].
The proposed method is especially adapted to the extraction of anomalies specified by intensity peaks in remote sensing data. The idea consists in modeling the image as a realization of a Gaussian field and determining a degree of belonging of the peaks to the field with respect to both radiometric and spatial characteristics. Such a principle has been used in functional MRI by Worsley, Friston and Poline. The proposed approach is based on their works, especially on [4, 9, 10].

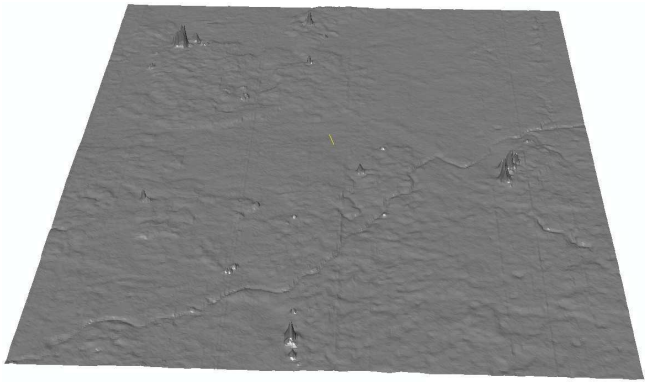

Figure 1: Height-map of a piece of TIR image

First, definitions and interesting properties concerning the Gaussian fields are mentioned. Then, a preprocessing is set up in order to consider the image as a realization of a Gaussian field. A statistical analysis allowing to detect the forest fires is presented in a third part. We then propose an extension to the estimation of the fire propagation direction. Finally, results are shown.
The proposed method is tested on TIR satellite images (BIRD satellite - 300 meter resolution) representing Portugal in May 2003.

2. GAUSSIAN FIELDS

In this section, definitions and properties related to the Gaussian field theory are presented. More details are available in [1] and [5].

Definition 1 *Let $(\Omega, \mathcal{F}, P)$ be a complete probability space and $\mathcal{T} \subset \mathbb{R}^N$ a topological space. A N-dimensional real valued random field is a measurable mapping $X : \Omega \rightarrow \mathbb{R}^{\mathcal{T}}$.*
X is homogeneous if $\forall \tau, t_1, ..., t_k \in \mathbb{R}^N$, the vector $(X(t_1), ..., X(t_k))$ follows the same distribution that the vector $(X(t_1+\tau), ..., X(t_k+\tau))$.

The collection of measures $F_{t_1,...,t_n}$ defined by $F_{t_1,...,t_n}(B) = P((X(t_1), ..., X(t_n)) \in B)$ where $B \in \mathbb{B}^n$ ($\mathbb{B}$ is a Borelian of

$\mathbb{R}$) is called the family of the $\mathscr{F}_d$ (finite dimensional) distributions.

Definition 2 *A random field is Gaussian if its $\mathscr{F}_d$ distributions are Gaussian vectors.*

Definition 3 *Let $F(t) : \mathbb{R}^N \rightarrow \mathbb{R}$ be a function. $\forall u \in \mathbb{R}$ and $S \subset \mathbb{R}^N$, the excursion set of F in S over the threshold u is defined by :*

$$A_u(F,S) = \{t \in S : F(t) \geq u\} \quad (1)$$

In imagery, A_u represents the set of clusters of an image F at the threshold u (see Figure 2). Adler [1] proposes an estima-

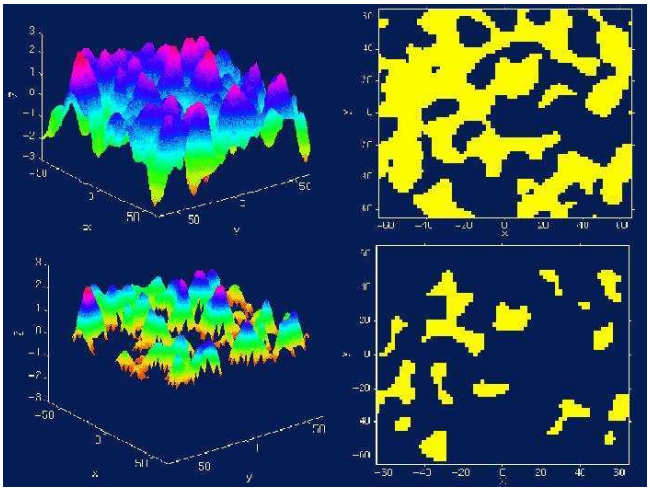

Figure 2: A realization of a 2-dimensional random field (left) associated with 2 excursion sets at different thresholds (right)

tion of the number m_u of clusters in the excursion set A_u. For a 2-dimensional homogeneous Gaussian field (centered and reduced), the expectation of m_u is given by:

$$E[m_u] = S(2\pi)^{\frac{3}{2}}|\Lambda|^{\frac{1}{2}} exp - \frac{u^2}{2} \quad (2)$$

where S represent the volume of the field (i.e the number of pixels in the image) and Λ, the covariance matrix of the field derivatives. This matrix allows to characterize the smoothness of the field.
This equation is a key point in the proposed method. However, in order to be able to use it in the imagery domain, the image must verify some hypothesis. In particular, the image must be modeled as a realization of a homogeneous Gaussian field. To do so, we approximate a Gaussian field by considering its $\mathscr{F}_d$ distributions as Gaussian. It represents an acceptable approximation since the covariance matrix Λ has a minor importance in the algorithm that we propose. In other words, the pixel distribution of the image must, by approximation, be Gaussian (i.e. the image histogram must be Gaussian).

3. PREPROCESSING

Preprocessing must be applied on the image in order to satisfy equation (2). The image must be modeled as a realization of an homogeneous Gaussian field, which imposes that at least the pixel distribution must be well approximated by a Gaussian law.
To do so, the first step consists in separating the various image modes (ground, clouds, sea,...) and in keeping the mode which have the highest intensity mean (i.e. the "ground" mode which is the closest to pixels representing forest fires). An iterated "2-means" algorithm, detailed in [5], is used to extract the mode of interest. The obtained sub-image has a unimodal distribution which includes potential forest fires. The forest fires are supposed to be rare events which means that their surface is negligible with respect to the surface associated with the considered mode. This hypothesis, which is necessary to obtain a correct separation of the modes, is acceptable since the complete TIR images represent vast areas of countries such as Portugal.
Then, the obtained class is regularized by using mathematical morphology. This regularization allows to delete the isolated elements of the class and "to fill in the holes".
Finally, the last stage consists in normalizing the resulting distribution by a histogram specification. The obtained sub-image has a pixel distribution which is Gaussian. So, This sub-image can be considered, by approximation, as a realization of an homogeneous Gaussian field.
These three stages are illustrated in Figure 3 where both the histogram of the image and a piece of the image are shown for each preprocessing steps.

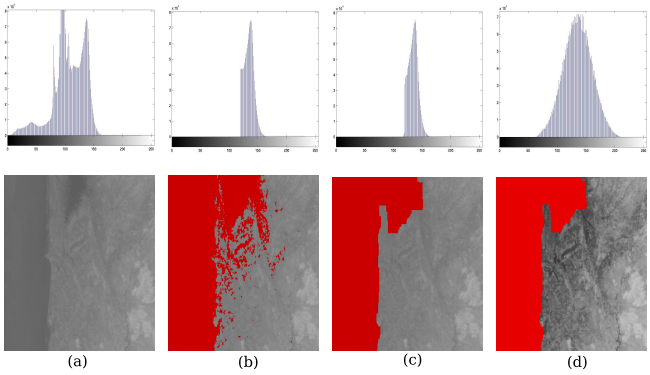

Figure 3: Preprocessing steps - **(a):** initial histogram of the complete image (top) associated with a piece of the image (bottom) - **(b):** extraction of the mode of interest - **(c):** regularization of the extracted mode **(d):** histogram specification by a Gaussian distribution

4. STATISTICAL ANALYSIS

The forest fires correspond to intensity peaks in the sub-image obtained in the previous section. The idea consists in considering this sub-image as a background (which is represented by a realization of a Gaussian field) where some anomalies (i.e. intensity peaks which represent forest fires) can exist. In this context, results concerning the Gaussian field theory, especially the equation (2), can allow to estimate whether a cluster belongs to the realization of a Gaussian field (i.e. the background). To do so, both radiometric and spatial information related to the cluster are used to define probabilities of belonging.

4.1 Radiometric information

The belonging of a cluster to the background can be estimated in function of the maximal intensity of this cluster. Let us consider $C_u^{x_0}$, a cluster at the threshold u having a maximal intensity x_0 (see Figure 4 - (left)). In the following, a cluster established at the threshold u is called a u-cluster. The probability that $C_u^{x_0}$ belongs to the realization of a Gaussian field (noted $\mathscr{B}$ as background) is given through the equation (2) by the expectation of the number of x_0-clusters to the expectation of the number of u-clusters ratio:

$$P(C_u^{x_0} \in \mathscr{B}) = \frac{E[m_{x_0}]}{E[m_u]} = \frac{x_o}{u} \exp \frac{u^2 - x_0^2}{2} \tag{3}$$

This probability is noted P_H. The behavior of P_H in function of u is particularly interesting: it has an unique minima which allows to fix a reference threshold u_0. In the following, this threshold allows to extract all the clusters which correspond to potential forest fires. More details about the computation of u_0 are available in [5].

4.2 Spatial information

The spatial characteristics of a cluster and more precisely its surface can also allow to estimate whether the cluster belongs to the background.
Let N_u be the number of pixels with an intensity superior to u, m_u be the number of u-clusters , and n_u be the surface (i.e. the number of pixels) of a u-cluster. Nosko [8] has established that n_u follows an exponential distribution. We aim at estimating the parameter of this exponential distribution, i.e. the inverse of the expectation of n_u. These variables are linked by the following expression [4]:

$$E[n_u] = \frac{E[N_u]}{E[m_u]} \tag{4}$$

The pixel distribution is Gaussian, so the expectation of N_u is given by:

$$E[N_u] = S \int_u^{\infty} (2\pi)^{-\frac{1}{2}} e^{-\frac{x^2}{2}} dx = S\Phi(-u) \tag{5}$$

The equation (2) allows to estimate the expectation of m_u. Then, the expectation of n_u can be expressed by the following equation:

$$E[n_u] = \frac{E[N_u]}{E[m_u]} = \frac{\Phi(-u)}{(2\pi)^{\frac{3}{2}} |\Lambda|^{\frac{1}{2}} exp - \frac{u^2}{2}} \tag{6}$$

Let us consider $C_u^{n_0}$, a u-cluster having a surface n_0 (see Figure 4 - (left)). The probability that $C_u^{n_0}$ belongs to the background corresponds to the probability that n_u is superior to n_0:

$$P(C_u^{n_0} \in \mathscr{B}) = P(n_u \geq n_0) = e^{-\frac{n_0}{E[n_u]}} = e^{\frac{(2\pi)^{\frac{3}{2}} |\Lambda|^{\frac{1}{2}} n_0 exp - \frac{u^2}{2}}{\Phi(-u)}} \tag{7}$$

This probability is noted P_S. In practice, Λ is computed using the empirical estimators of the variances and co-variances of the field derivatives.

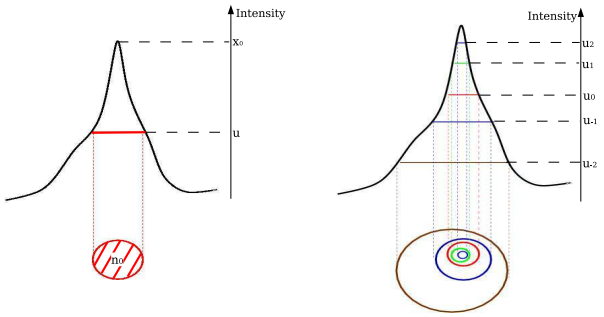

Figure 4: **Left:** Scheme of a u-cluster having a maximal intensity x_0 and a surface n_0 (profile and top views of the intensity peak) - **Right:** Family of sub-clusters and sup-clusters related to the threshold family U

4.3 Algorithm

The probabilities P_H and P_S allow to estimate the belonging of a cluster to the background using two different characteristics of this cluster (i.e. its maximal intensity and its surface). We aim at defining a decision law taking into account both probabilities.
This decision law consists in considering the cluster as foreigner to the background if:

$$\min(P_H, P_S) < \alpha \tag{8}$$

where α is the limit probability, i.e. a confidence coefficient on the result which acts as a "P-value". In practice, α is close to 10^{-2}. This decision law mainly relies on the probability P_H (i.e. on the radiometric characteristic of the cluster). The probability P_S is tested only if the test on P_H is rejected.
The decision law allows to locally analyze a cluster. We aim at defining a global algorithm dealing with the complete image. First, we extract all the clusters at the threshold u_0 (defined in section 4.1) which correspond to potential forest fires. Then, each detected cluster is extended to a family of sub-clusters with respect to the family of thresholds $U = (u_{-k}, ..., u_0, ..., u_k)$. This extension allows to have a better precision concerning the location of forest fires. In practice, we take $k = 2$ (see Figure 4 - (right)). Finally, the decision law is applied to all these clusters. This algorithm is summed-up as follows:

Algorithm 1 .

1. *Fix the limit probability α,*
2. *Extract the set of u_0-clusters,*
3. *For each detected cluster,*
   - Establish the family of clusters w.r.t. the threshold set U,
   - For each element of this family, compute P_S and P_H,
4. *Keep the cluster accepted by the decision law (equation (8)).*

5. ESTIMATION OF THE FIRE PROPAGATION DIRECTION

The detected areas can provide additional information by studying the topography of their intensity peaks. Figure 5 represents the typical topography of an intensity peak

corresponding to a forest fire. This peak is composed of two parts. The first one represents the pixels of very high intensity (right side) which present high discontinuities with the neighboring pixels: it corresponds to the fire fronts. The second part (left side) represents lower intensity pixels which refers to the burned area. By considering the alignment of these two areas, the fire propagation direction can be estimated. It provides interesting information related to the evolution of the fires, which can be useful for firebrigades for instance.

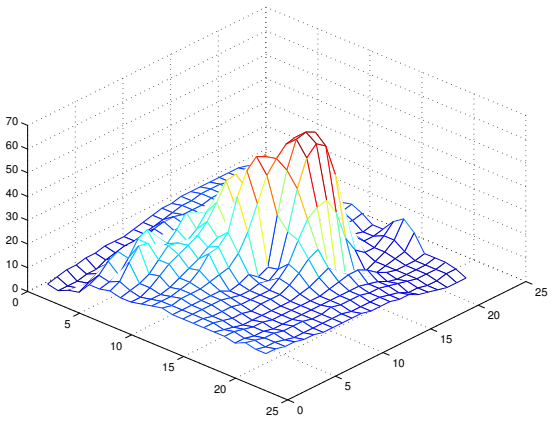

Figure 5: Typical topography of an intensity peak corresponding to a forest fire

In order to estimate the fire propagation direction, we propose a very simple but efficient process which consists in comparing the intensity weighted center to the spatial center of the cluster. Let C be the spatial center of a cluster and M, its intensity weighted center (i.e. $M = \frac{\sum_s s \times x_s}{\sum_s x_s}$ where the s and x_s are respectively the pixels and the pixel intensities of the cluster). The fire propagation direction $\widehat{\theta}$ is estimated by the following expression:

$$\widehat{\theta} = \arg(\overrightarrow{CM}) \tag{9}$$

where arg is the argument of a 2D-vector. The value of the modulus of $\overrightarrow{CM}$ can be seen as a confidence coefficient on the estimated orientation. Figure 7 shows results obtained on different clusters. We remark that neighboring clusters have similar orientations. It can be explained by the local influence of the wind in the propagation of the forest fires.

6. RESULTS

The proposed approach has been tested on TIR satellite images (BIRD satellite - 300 meter resolution - 1000×4000 pixels) representing Portugal acquired at various dates of May 2003.
Figure 8 shows a result on a piece of image associated with the ground truth. On the ground truth (which has a lower quality), the white clusters (corresponding to forest fires) have been voluntarily enlarged in order to make a better distinction. 16 forest fires are present on the ground truth. We detect 15 of the 16 forest fires with a confidence coefficient $\alpha = 0.05$. One false alarm is located. This result is convincing compared to results obtained by [3].

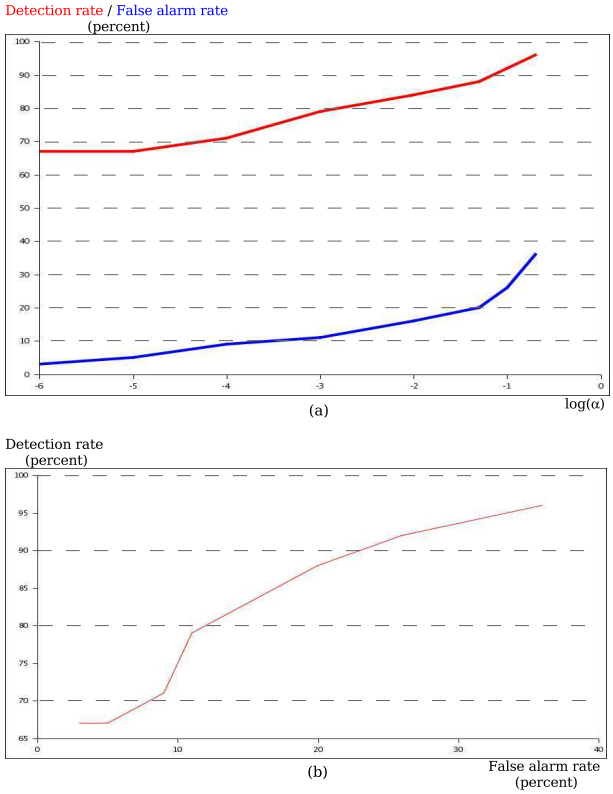

Figure 6: **(top):** Detection rate (red) and false alarm rate (blue) vs the confidence coefficient α - **(bottom):** the corresponding ROC curve

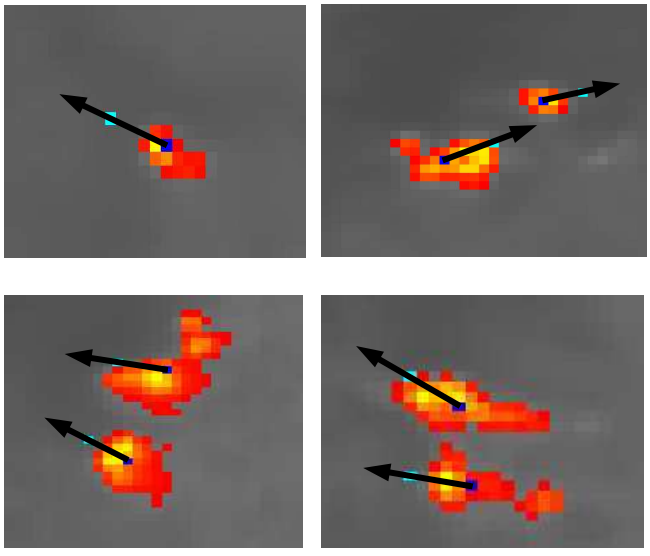

Figure 7: Various clusters detected as forest fires (red to yellow : intensity value) associated with the estimation of their propagation direction (black arrow)

Generally speaking, Figure 6 presents the detection rate and false alarm rate (in term of number of clusters) in function of the confidence coefficient. This figure also shows the ROC (Receiver-Operator Characteristics) curve. The optimal performances are obtained for a confidence coefficient contained between 0.05 and 0.01. For instance, $\alpha = 0.01$ allows to detect 85% of the forest fires with 15% of false alarms.

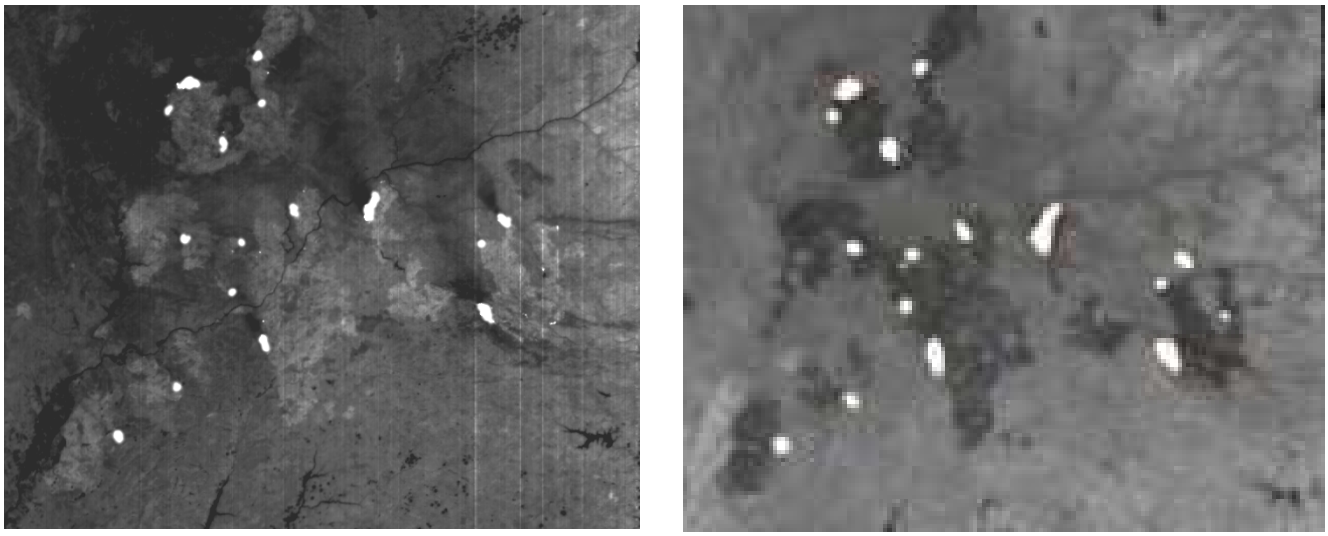

Figure 8: **(left):** Extract of the result obtained on a TIR image (BIRD ©DLR), white clusters represent the detected forest fires - **(right):** ground truth provided by Alcatel Alenia Space

However, the choice of α mainly depends on the application. For example, firemen will prefer a low confidence coefficient (i.e. detecting as many forest fires as possible even if many false alarms are located).
The computing time is acceptable: two minutes are necessary to detect the forest fires using a 2Ghz processor on a 1000×4000 image (i.e. an area corresponding to the surface of Portugal).

7. CONCLUSION

The proposed method allows to automatically extract the forest fires from TIR satellite images. The results only depend on α which acts as a confidence coefficient. Both detection rate and false alarm rate provide convincing values. Interesting information, related to the evolution of the fires, can also be obtained through the estimation of fire propagation direction.
However, the radiometric and spatial information, which allow to define the decision law, are set up independently. It could be interesting to introduce the probability $P(C_u^{x_0,n_0} \in \mathscr{B})$ (i.e. the probability that a u-cluster having both a maximal intensity x_0 and a surface n_0 belongs to the background) in the decision law in order to get a more robust method. In the future, we should work on this point.

8. ACKNOWLEDGMENTS

The authors thank the German Aerospace Center (DLR) and Alcatel Alenia Space for respectively providing the data and the ground truth.

REFERENCES

[1] R.J. Adler. *The Geometry of Random Fields*. Wiley, 1981.

[2] M.J. Carlotto. A cluster-based approach for detecting man-made objects and changes in imagery. *IEEE Trans. on Geoscience and Remote Sensing*, 43(2):374–387, 2005.

[3] M. Flannigan and T. Vonder Haar. "Forest fire monitoring using NOAA satellite AVHRR". *Canadian Journal of Forest Research*, 16:975–982, 1986.

[4] K.J. Friston, K.J. Worsley, R.S.J Frackowiak, J.C Mazziotta, and A.C. Evans. "Assessing the significance of focal activations using their spatial extent". *Hum. Brain Map.*, 1:214–220, 1994.

[5] F. Lafarge, X. Descombes, and J. Zerubia. Détection de feux de forêt par analyse statistique de la radiométrie d'images satellitaires. Research Report 5369, INRIA, France, December 2004.

[6] F. Lafarge, X. Descombes, and J. Zerubia. Textural kernel for SVM classification in remote sensing : Application to forest fire detection and urban area extraction. In *Proc. IEEE International Conference on Image Processing*, Genoa, Italy, September 2005.

[7] Y. Li, A. Vodacek, R.L. Kremens, A.E. Ononye, and C. Tang. A hybrid contextual approach to wildland fire detection using multispectral imagery. *IEEE Trans. on Geoscience and Remote Sensing*, 43(9):2115–2126, 2005.

[8] V.P. Nosko. "Local structure of Gaussian random fields in the vicinity of high level shines". *Soviet Mathematics : Doklady*, 10:1481–1484, 1969.

[9] J-B. Poline, K.J. Worsley, A.C. Evans, and K.J. Friston. "combining spatial extent and peak intensity to test for activations in functional imaging". *NeuroImage*, 5:83–96, 1997.

[10] K.J. Worsley, S. Marrett, P. Neelin, and A.C. Evans. A three-dimensional statistical analysis for CBF activation studies in human brain. *Journal of Cerebral Blood Flow and Metabolism*, 12:900–918, 1992.